Journal of Applied Fluid Mechanics, Vol. 10, No. 3, pp. 989-999, 2017.
Available online at www.jafmonline.net, ISSN 1735-3572, EISSN 1735-3645.
DOI: 10.18869/acadpub.jafm.73.240.27314

Numerical Investigation of the Performance of Kenics Static Mixers for the Agitation of Shear Thinning Fluids

A. Mahammedi[1,2], H. Ameur[3†] and A. Ariss[1]

[1] *Polytechnic National School of Oran (ENPO), 31000, Algeria*
[2] *Mechanical Engineering Research Laboratory (LaRTFM), Polytechnic National School of Oran (ENPO) PB 1524, El-M'Naouar, Oran 31000, Algeria*
[3] *Department of Technology, Institute of Science and Technology, Ahmed Salhi University Center of Naâma (Ctr Univ Naâma), PB 66, 45000, Algeria.*

†*Corresponding Author Email:houari_ameur@yahoo*

(Received October 22, 2016; accepted December 31, 2016)

ABSTRACT

The laminar flow of non-Newtonian fluids through a Kenics static mixer is investigated by using the CFD (Computational Fluid Dynamics) tool. The working fluids have a shear thinning behavior modeled by the Ostwald De Waele law. We focus on the effect of Reynolds number, fluid properties, twist angle and blade pitch on the flow characteristics and energy cost. The pressure drop information obtained from the simulations was compared to several experimental correlations and data available in the literature. The numerical results were found in good agreement with the experimental values. From the obtained results, the twist technique is confirmed to be very useful to enhance the mixing with less power consumption and at low Reynolds numbers. A faster axial mixing has been achieved with increased blade length and decreased twist angle. However, the good mixing near the tube walls was obtained with increased twist angle. The power consumption expressed in power drop was found to be increase with increased CMC concentrations, Reynolds number, twist angle and decreased blade length.

Keywords: Static mixer; Kenics mixer; Non-newtonian fluids; Twist angle; Blade length.

NOMENCLATURE

D	tube diameter	V_{in}	inlet velocity
K	fluid consistency	X	axial coordinate
l	length of the element	X^*	dimensionless axial coordinate
L	length of the tube	Z	Pressure drop ratio, dimensionless
n	flow index		
Q	flow rate	α	angle of twist blade
R	mixer radius	ΔP	pressure drop
R^*	dimensionless mixer radius	ΔP_{EM}	pressure drop for empty tube
Re_g	Reynolds number for a shear thinning fluid = (Eq. 6)	ΔP_{SM}	pressure drop for static mixer
		μ	dynamic viscosity of fluid
U^*, V^*, W^*	dimensionless velocity	ρ	density of fluid
U, V, W	axial, radial, tangential velocity, respectively		

1. INTRODUCTION

In nearly all industrial chemical processes, like as homogenization, gas dispersion, crystallization and polymerization, the mixing plays an important role on the final product quality. Inefficient mixing results in a lower product quality with increased production cost. Therefore, determining the mixing characteristics is extremely important, especially for highly viscous non-Newtonian fluids, where the chance of the presence of poorly or isolated mixed zones is high. Until present, many researchers

continue to investigate the efficiency of different mixing systems (Ameur, 2015, 2016a; Khapre and Munshi, 2015; Kazemzadeh *et al*., 2016).

Kenics static mixers, also known as motionless mixers (Thakur *et al*., 2003), are widely encountered in many industries, such as the, petroleum, pharmaceutical, paint and food industries for achieving a wide range of operations such as power generation, chemical reaction, refining, air-conditioning and gas treatment (Bi *et al*., 2013; Li *et al*., 2011; Kroon and Hartmann, 2008).

However, instead of realizing many operations in stirred tanks, it is more interesting to achieve mixing in feed lines by static mixers, because reduced equipment cost and space are required. Another interesting advantage is the power consumption, the required power comes directly from the pump which drives the inline flow and no extra motor drive is needed. Also, static mixers are preferred for their good mixing quality at low shear rates, low equipment cost, small space requirement, sharp residence time distributions, self-cleaning capability and high interfacial area production (Thakur *et al*., 2003; Etchells and Meyer, 2004; Ghanem *et al*., 2014). Static mixers are also good alternatives for processing aggressive and corrosive media, and for high pressure operations, where shaft feed troughs are expensive (Rabha *et al*., 2015). Static mixers are also used to improve the mass transfer rates from gas to liquid (Goto and Gaspillo, 1992; Heyouni *et al*., 2002; Martin and Galey, 1994; Munter, 2010).

Among all kinds of static mixers, the Kenics mixers designed by Sulzer Ltd, are widely used in the mixing of high viscous fluids and fluids with extremely diverse viscosity especially in polymer processing. The design of the mixer consists of a cylindrical pipe equipped with a number of helical blade elements. Each blade is positioned perpendicular to the preceding one, is twisted to the right or left by a degree of 180° twist. The mixing is ensured by stretching and reorientation of fluid during its passage through the blade: the twist and perpendicular cut delivers a sequence of folding and stacking (Rafiee *et al*., 2013).

Meng *et al*. (2014) studied numerically the mixing performance of static mixers with multi-twisted leaves like Kenics mixer. Meijer *et al*. (2012) achieved a quantitative comparison of static mixers. Zhang *et al*. (2015) combined Kenics and SMX mixers for mixing polyacrylamide solutions, and they found that this combination has a good performance. Olmiccia *et al*. (2011) studied the residence time distribution in a Kenics static mixer. Other researchers used numerical methods to characterize the stretching histories and the flow fields in two and three-dimensions (Hobbs *et al*., 1998; Hobbs and Muzzio, 1998; Galaktionov *et al*., 2003; Kumar *et al*., 2008). Rafiee *et al*. (2013) used the Positron Emission Particle Tracking (PEPT) technique to visualize the flow in a Kenics mixer for Newtonian and non-Newtonian fluids in the laminar regime. They reported that the non-Newtonian fluid flow requires a shorter length to develop than the Newtonian fluid. The above mentioned papers and others (Barega *et al*., 2013; Jin and Cheng, 2011), confirm that the static mixer, when compared with a conventional impeller, can yield a more controlled and scalable rate of dilution in fed batch system and also homogenize feed streams with a minimum residence time with less power consumption.

For a Kenics mixer, Saatdjian *et al*. (2012) reported that the initial location of a blob of dye is important for its spreading over the cross section of the tube only in the first few mixing elements, its influence decreases afterwards. The eccentric position of helical elements may improve slightly the mixing efficiency by increasing the extensional efficiency of mixing and giving a more homogeneous distribution of stretching rates inside the Kenics mixer (Saatdjian *et al*., 2012).

There are very few studies in the literature on non-Newtonian liquid mixing with static mixers. Thus, the purpose of the present study is to investigate the effect of some parameters on the performance of a Kenics static mixer for mixing shear thinning fluids. Aiming to have a static mixer with a smaller degradation rate, lower energy consumption and pressure drop, with good mixing quality, four parameters are studied, namely: the twist angle, the blade pitch the flow rate and fluid rheological properties.

2. GEOMETRY SIMULATED

Geometry of the model simulated (Fig. 1) is based on the Kenics KM static mixer manufactured by Chemineer (Dayton, OH). It consists of a tube with a diameter D = 0.01 m and a length L = 0.12 m. Each element has a thickness t = 1 mm. The first and the final helical blade elements are placed at the same distance l_1 = 0.015 m from the tube inlet and the tube outlet, respectively. The effect of blade twist (α) is investigated and three geometrical configurations are realized for this purpose, which are: α = 30°, 60° and 90°. The effect of blade length (l) is also explored by creating three other geometries, which are $l^* = l/L$ = 0.10, 0.15 and 0.20.

The fluid simulated (Carboxy Methyl Cellulose (CMC)) has a shear thinning behaviour. According to measures achieved by Gopal *et al*. (2015), the rheological properties of CMC solutions employed in the present study are summarized in Table 1.

Table 1 Rheological properties of the working fluid

	Concentration C (g CMC/g)	K (Pa s^n)	n
Solution No. 1	0.04	0.79	0.83
Solution No. 2	0.05	2.55	0.75
Solution No. 3	0.06	3.83	0.74

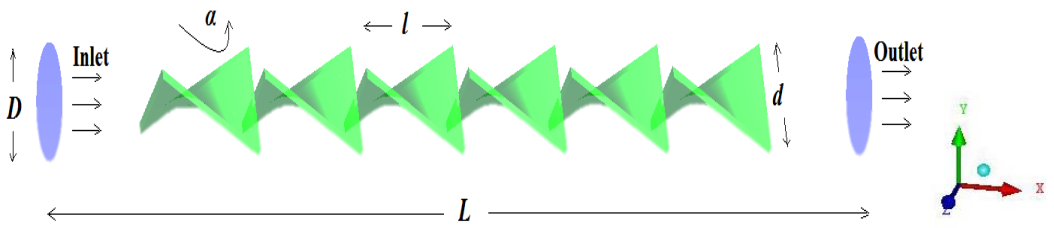

Fig. 1. Kenics static mixer.

3. MATHEMATICAL EQUATIONS

The governing equations of mass and momentum conservation used to solve the incompressible and isothermal flow problems are given as:

$$\nabla u = 0 \tag{1}$$

$$\frac{\partial \rho u}{\partial t} + \nabla .(\rho u u) = -\nabla p + \nabla \tau \tag{2}$$

where u is the velocity vector, ρ is the fluid density, τ is the stress tensor and p is the pressure.

In the present work, the stress tensor for the non-Newtonian fluid tested was described by the Ostwald–De Waele relationship:

$$\tau = k \dot{\gamma}^{n} \tag{3}$$

Where $\dot{\gamma}$ is the shear rate

We recall that for a Newtonian fluid flow in a pipe, the Reynolds number is defined by:

$$Re = \frac{\rho u D}{\mu} \tag{4}$$

Where D is the cylindrical pipe diameter and μ is the dynamic viscosity.

In the case of non-Newtonian fluid flows, the apparent viscosity for the so-called power-law fluid is given by:

$$\mu = k \dot{\gamma}^{n-1} \tag{5}$$

The generalized Reynolds number (Re_g) for a shear thinning fluid (Ostwald model) is defined as:

$$Re_g = \frac{\rho u^{2-n} D^{n}}{k} \tag{6}$$

Or, according to Rudman *et al*. (2004):

$$Re_g = \frac{\rho u^{2-n} D^{n}}{\frac{k}{8}\left(\frac{6n+2}{n}\right)^{n}} \tag{7}$$

where k is the consistency index and n is the power law index. We define the following dimensionless variables:

$$X^* = X/L \tag{8}$$

$$R^* = 2R/D \tag{9}$$

$$U^* = U/Vin \quad ; V^* = V/Vin \quad ; W^* = V/Vin \tag{10}$$

Where V_{in} is the inlet velocity. U, V and W are the axial, radial and tangential velocity components, respectively.

4. NUMERICAL METHOD

In this article, the geometry of the problem studied was created by the computer tool Ansys ICEM CFD (version 16.0). The computational domain was then divided into tetrahedral meshes by the same software (Fig. 2). Refined mesh was created near the tube wall and helical elements to capture the flow details. Mesh tests were performed by checking that additional cells did not change the velocity in regions with high magnitudes by more than 2.5%, as achieved by other authors (Ameur, 2016b). After mesh tests (Table 2), the case with the total number of elements of 544,817 was selected as the best, since it combines between the high accuracy of results and the lower time required for convergence. The selected mesh (i.e. the computational domain) was then exported to the computer tool Ansys CFX (version 16.0). The boundary conditions (inlet, outlet and walls) are defined in the CFX-pre-process. All solid boundaries were defined as stationary walls, with no-slip conditions applied. Different Reynolds numbers for the flow inside the pipe were obtained by varying the mass flow rate at the inlet boundary. All simulations were carried out for a steady state. The fluid is assumed to be incompressible and non-Newtonian (shear thinning) and all required properties of the working fluid are given in Table 1.

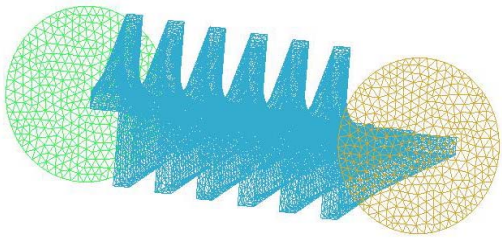

Fig. 2. Tetrahedral mesh of the computational domain.

The flow regime was laminar (the Reynolds number (Re_g) is ranged between 0.1 and 150). The process was considered stationary and isothermal.

Calculations were performed on a machine with a 2.20 GHz Pentium(R) i7 Core CPU with 12.0 GB of RAM. Simulations were considered to be converged when the residual target of mean velocities and pressure drop below 10^{-7}. Convergence was obtained after about 800÷1000 iterations and about 4÷5 h.

Table 2 Mesh tests performed

	M1	M2	M3
Number of grids	325,569	544,817	856,892
Pressure drop [Pa]	$8.7161 \cdot 10^4$	$8.7167 \cdot 10^4$	$8.7169 \cdot 10^4$
CPU time [seconde]	15,589	25,847	33,512

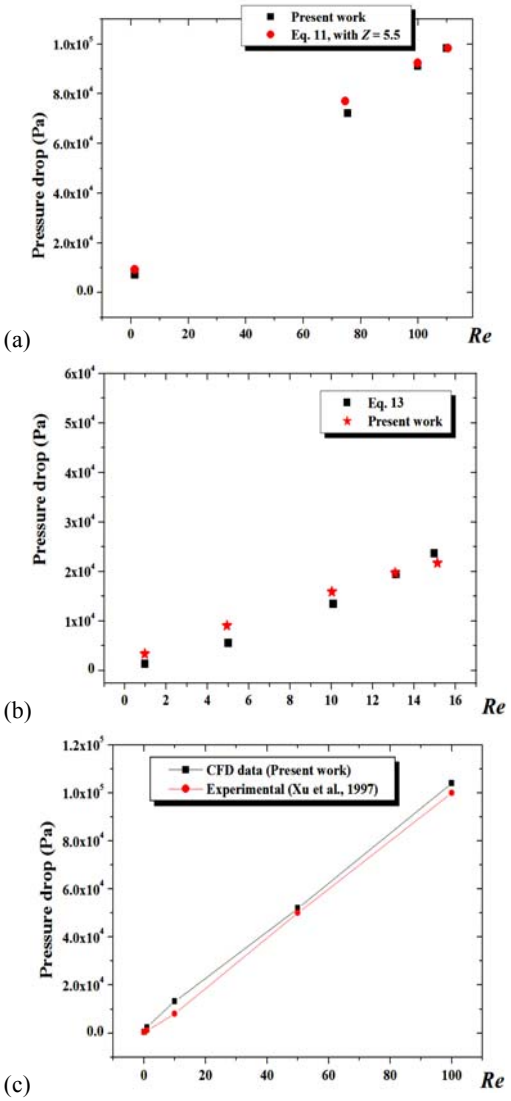

Fig. 3. Pressure drop vs. Reynolds number.

5. VALIDATION

Values of the pressure drop obtained via numerical simulations were compared with the values calculated by using known experimental correlations. The majority of these correlations are written in terms of a *Z*-factor and Reynolds number, as:

$$Z = \frac{(\Delta P)_{mx}}{(\Delta P)_{ep}} \tag{11}$$

where $(\Delta P)_{ep}$ is the pressure drop in the empty pipe and $(\Delta P)_{mx}$ is the pressure drop along the static mixer. The pressure drop per unit length without a static mixer is obtained by solving the Stokes equations:

$$\frac{(\Delta P)_{ep}}{L} = \frac{32}{Re}\frac{\rho V^2}{D} \tag{12}$$

Wilkinson and Cliff (1977) have proposed a correlation for the pressure drop in Kenics mixers:

$$Z = 7.19 + \frac{32}{Re} \tag{13}$$

and Grace (1971) has suggested another correlation:

$$Z = 3.24(1.5 + 0.21\sqrt{Re}) \tag{14}$$

For the laminar flow, The pressure drop obtained from CFD simulations was compared to several experimental correlations available in the literature (Figs. 3a, 3b). Another validation with the experimental data of Xu *et al*. (1997) is made and presented in Fig. 3c). As remarked on the three figures, a good agreement is obtained.

6. RESULTS AND DISCUSSION

6.1. Flow fields and Pressure Distribution

In the first part of our investigation, we present the distribution of flow fields and pressure in different locations of the mixer (Figs. 4, 5 and 6). We note that the results presented in this section are obtained for a Kenics mixer with six elements, the length of each element ($l^* = l/L$) is equal to 0.1 and each element is twisted by an angle $\alpha = 90°$.

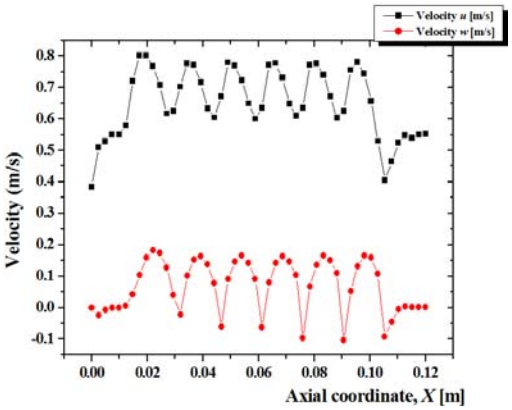

Fig. 4. Axial and radial velocity profiles vs. the axial coordinate, Re_g = 10, solution No. 1, $R^* = 2R/D$ = 0.12, l^* = 0.10, α = 90.°

For a radial position $R^* = 2R/D = 0.12$, the axial and radial velocities are presented along the mixer length (Fig. 4). First, we remark that both velocity

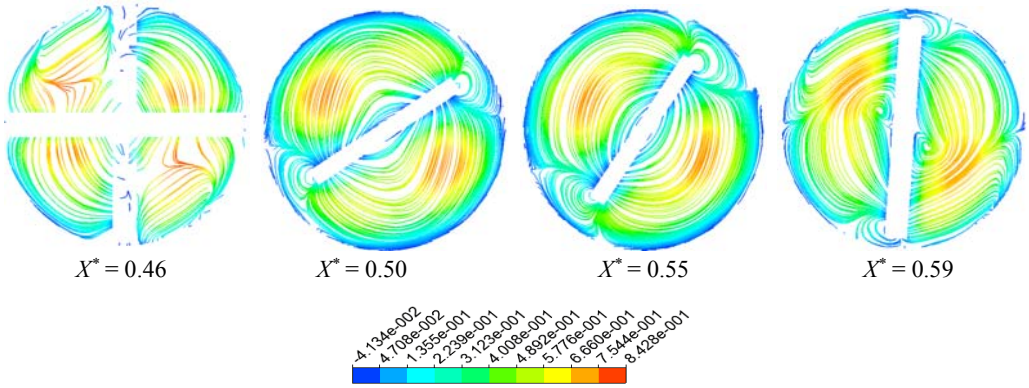

Fig. 5. Streamlines for Re_g = 150, Solution No. 1, l^* = 0.10, α = 90°.

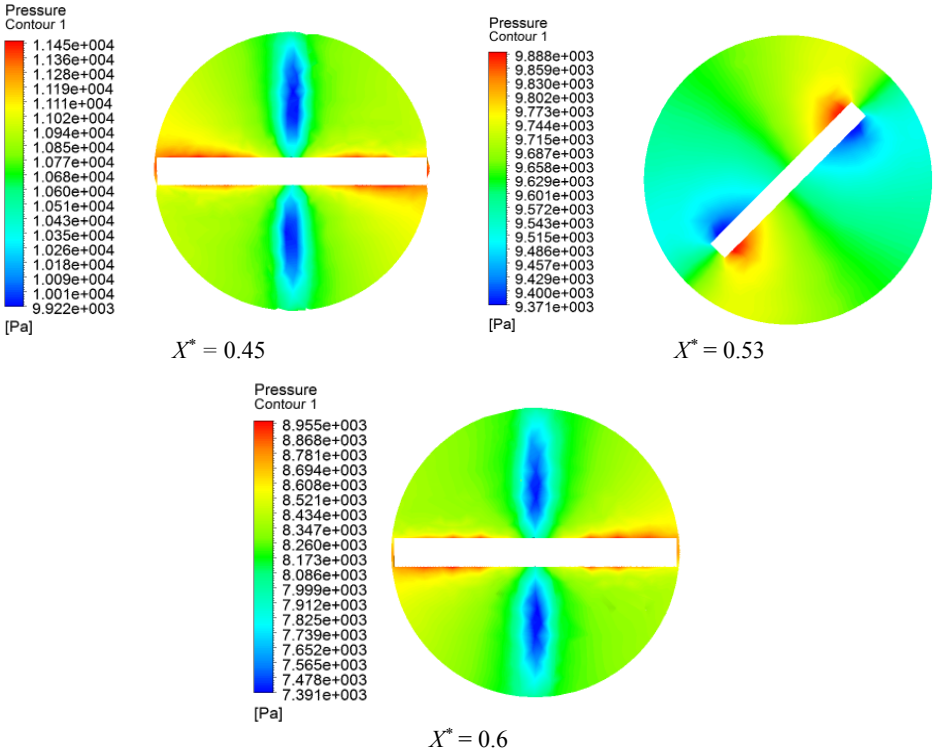

Fig. 6. Pressure distribution at the 3rd element for Re_g = 10, Solution No. 1, l^* = 0.10, α = 90°.

components increase continually until they reach their maximum at the middle of the length element, then they decrease until their minimum values at the intersection of two neighbour elements. Next, the same velocity profile will be repeated for all mixer elements. Also, it should be mentioned that the axial velocity component is the dominant (compared to the radial component).

Since the flow is periodic, we have chosen one element (the third one) for the presentation of streamlines (Fig. 5) and pressure distribution (Fig. 6). In Fig. 5, X^* is the dimensionless axial position (X/L). We note that the axial coordinate (X^*) of the third element is limited between 0.45 and 0.65.

In Fig. 5, we remark that the twist shape of element creates more chaotic advection of fluid particles and a vortex is formed in the space between the element and pipe wall. This vortex increases in size with the increase of twist angle (i.e. when we advance with the element length). Furthermore, another vortex is formed at each side of the element for a position very close to the next element (i.e. close to the point of intersection of two neighbour elements). This is due to the sharp change in geometry, since the angle between the end of the each element and the beginning of the next one is 90°. The two factors: twist of element and the sharp change of angle between elements are responsible for intense movement of fluid particles and the good mixing.

Figure 6 shows the pressure at the 3rd element surface. A high pressure region is found where the high speed core coming from the previous element make a hit on the blade. The low pressure region is found where the fluid leaves the element.

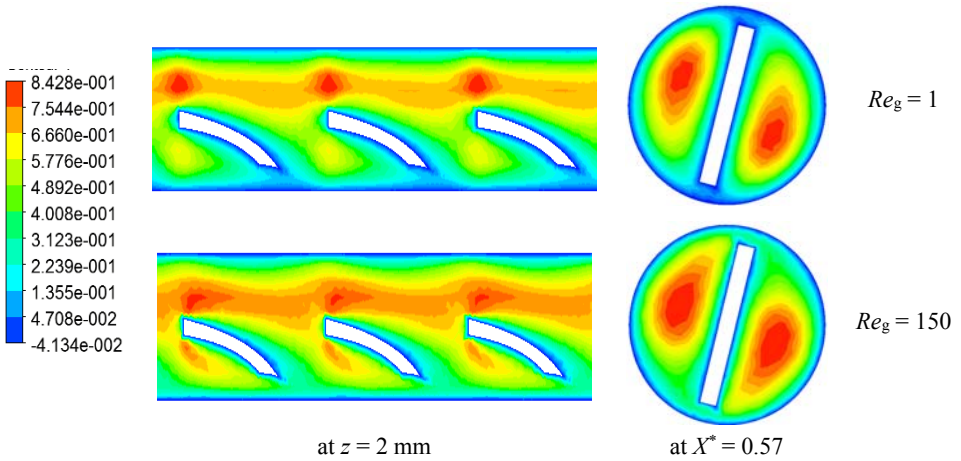

Fig. 7. Dimensionless velocity contours for Solution No. 1, l^* = 0.10, α = 90°.

6.2. Effect of Reynolds Number

In a simple tube and at low values of Reynolds number, trajectories of fluid particles are parallel to the pipe wall, the pressure per unit length is low and the mixing in a cross section is poor compared to the turbulent regime. With the increase of Reynolds number, the fluid flows are more intensified and the mixing in a cross section will be enhanced, but an additional penalty in pressure drop. An efficient solution for this issue is the use of static mixers, which are twisted elements inserted inside the pipe to cut, twist, fold and re-combine fluid particles (Hobbs and Muzzio, 1998). This design may create under laminar flow conditions a chaotic advection as in turbulent flows (Hobbs and Muzzio, 1997; Saatdjian *et al*., 2012).

A comparison of velocity contours for two different values of Reynolds number in the Kenics mixer reveals clear the impact of Reynolds number (Fig. 7).

The flow in a six-element static mixer has been analysed via dimensionless velocities (axial, radial and tangential velocity) vs. mixer radius. We remark that the axial velocity increases when Reynolds number increases. In reverse, values of the dimensionless velocity components adjacent to the tube wall are smaller with the higher Reynolds number (Fig. 8). The minus sign of radial and tangential velocities (Fig. 8b, 8c, respectively) indicate the existence of reverse flows. The increase of Re_g yields an increase in vortices.

Figure 9 shows the velocity streamlines for different Reynolds numbers (Re_g = 10, 50 and 150). For the deep laminar regime (Re_g = 10), no vortices are formed near the side of element. However and for higher Re_g (Re_g = 50), both primary and secondary vortices are observed clearly on both sides of the Kenics element. These vortices are more toroidal with increased Re_g. Also, the small vortex formed in the space between the element and the pipe wall at Re_g = 50 is increased when Re_g = 150.

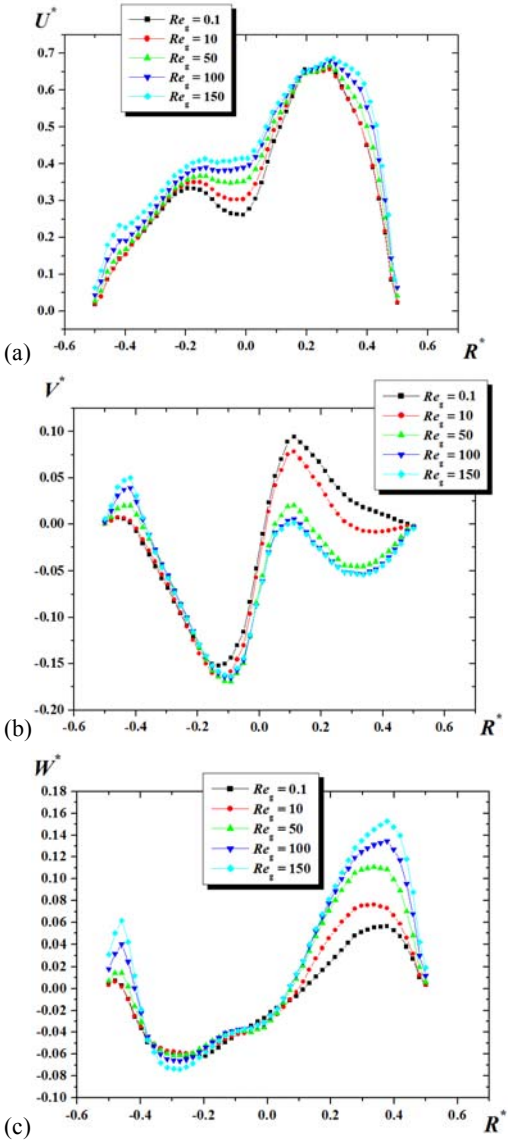

Fig. 8. Dimensionless velocities vs. mixer radius for Solution No. 1, X^* = 0.59, l^* = 0.10, α = 90° (a) axial velocity, (b) radial velocity, (c) tangential velocity.

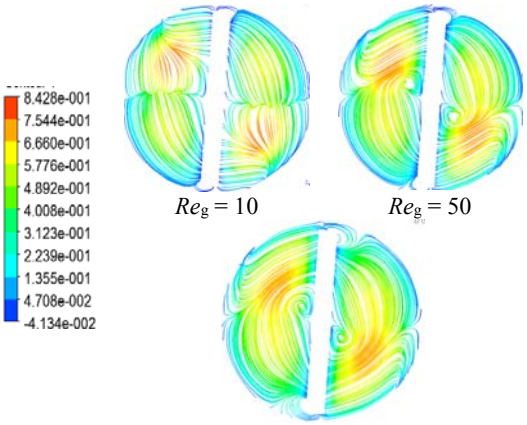

Fig. 9. Streamlines for different Reynolds numbers, Solution No. 1, X^* = 0.59, α = 90°.

As resumed in this section, the increase of flow rate (i.e. the Reynolds number) is advantageous to intensify the fluid movements and to enhance the mixing. However, what about the energy consumption? This issue is investigated in the following sections.

6.3. Effect of Fluid Rheology

Figs. 10, 11 and 12 show that the flow contours and the axial velocity distribution are relatively influenced by of the concentration level. Dilute CMC solutions leads to a very well mixed region. The well-mixed region presents the area where the interaction between fluid particles is intense, i.e. the region with high velocity magnitudes.

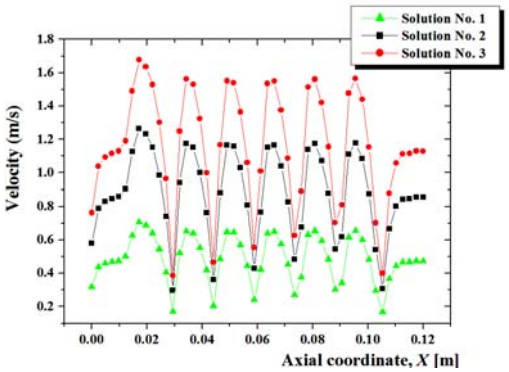

Fig. 10. Axial velocity component for the Kenics-mixer for different CMC samples, Re_g = 10, R^* = 0.2, l^* = 0.10, α = 90°.

The pressure drop across the static mixer is affected by the concentration level. The pressure drop increases significantly with increasing concentration level (Fig. 13). This figure shows also that the pressure drop rises as Reynolds number increases.

6.4. Effect of the Pitch Ratio

The blade design plays an important role on the power consumption and overall mixing characteristics. Here, we explore the effect of blade length expressed as the pitch ratio $l^* = l/L$. The faster flows are obtained with the great values of the pitch ratio (Fig. 14).

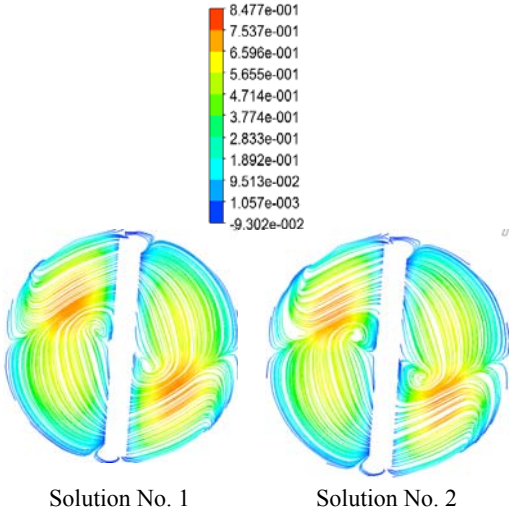

Fig. 11. Flow fields for Re_g = 75, l^* = 0.10, α = 90°.

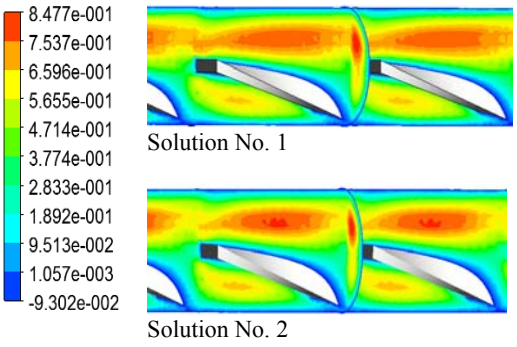

Fig. 12. Well mixed region, for Re_g = 75, l^* = 0.10, α = 90°.

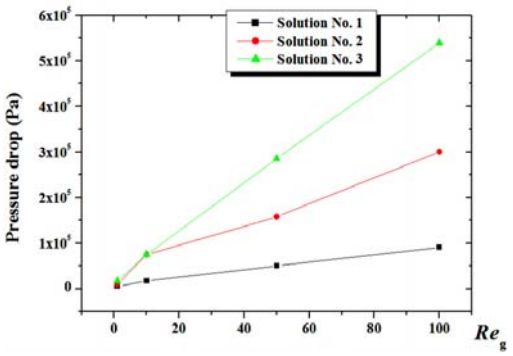

Fig. 13. Pressure drop vs. Reynolds number for different solutions, l^* = 0.10, α = 90°.

The comparison of pressure drops across the helical static mixer using three different values of the blade length ratio ($l^* = l/L$ = 0.1, 0.15 and 0.20) shows a significant increase in the pressure drop as Reynolds number increases and the blade length decreases (Fig. 15). This is due to the rise in the number of elements.

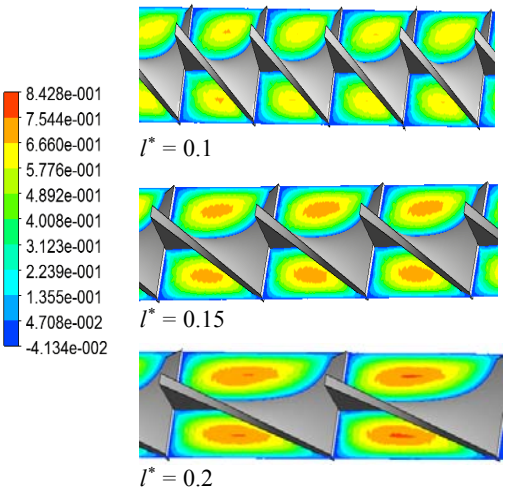

Fig. 14. Flow fields for different values of the blade length ratio $l^* = l/L$, Solution No. 1, $Re_g = 100$, $\alpha = 90°$.

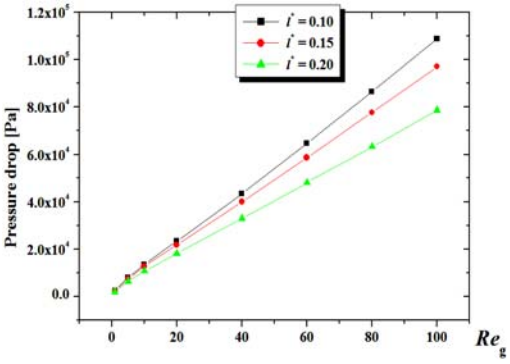

Fig. 15. Pressure drop for different values of the blade length ratio $l^* = l/L$, Solution No. 1, $\alpha = 90°$.

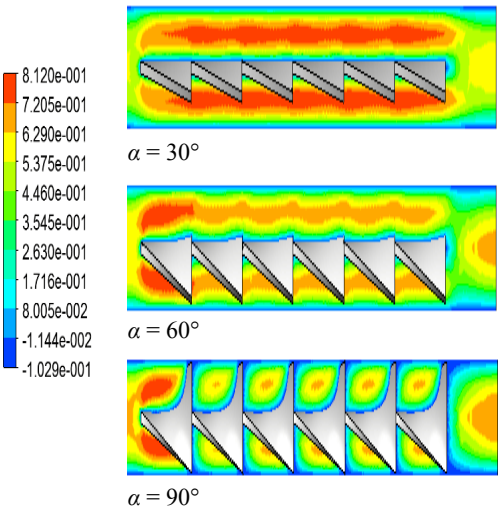

Fig. 16. Velocity contours for $Re_g = 100$, Solution No. 1, $l^* = 0.10$.

6.5. Effect of the Twist Angle

For a tube equipped with six elements ($l^* = 0.1$) and for three different values of the twist angle ($\alpha = 30°$, 60° and 90°), the velocity distribution is presented under various forms (a horizontal plane in Fig. 16 and a vertical plane in Fig. 17). The axial velocity profile develops rapidly into a parabolic profile (Fig. 18a) and the higher values are observed in the tube centre (Figs. 16, 17, 18a). The speed cores of the flow decrease with the augmentation in the twist angle from ٣0° to ٩0° (Figs. 16, 17).

The increase of twist angle generates an increase in the radial and tangential velocities and a decrease in the axial velocity. This is explained by the formation of vortex on both sides of blade for only the case $\alpha = 90°$. The presence of such vortices requires an additional power in terms of pressure drop (as observed in Fig. 19): the pressure drop augments with the augmentation of the twist angle from ٣0° to ٩0° over the range of Reynolds number ($1 \leq Re_g \leq 100$).

7. CONCLUSION

Using the numerical method described above, the flow and the dependence of mixing in a six-element static mixer has been analysed for a number of different flow conditions, fluid properties and geometrical parameters (twist angle, blade length) were investigated. Also the pressure drop was determined for all cases studied.

The velocity flow fields are likely to be quite different with different geometries. The CMC solutions, depending on their concentrations, revealed properties classic for shear thinning fluids.

The comparison of velocity fields revealed clear differences in the Kenics flows that the Reynolds number and concentration level of the non-Newtonian solution have a major impact on the performance of the helical static mixer.

The concluding remarks may be summarized as follows:

- The increased Reynolds number may intensify the chaotic advection of fluid particles and enhance mixing but with an additional consumption in power which is yielded by the high pressure drop.
- Faster flows may be obtained with increased blade length.
- The increase of twist angle generates an increase in the radial and tangential velocities and a decrease in the axial velocity.
- The faster axial mixing is achieved with the decrease of twist angle.
- The best mixing near the tube walls is obtained when vortices are formed on both sides of the blade, i.e. in the case of the twist angle $\alpha = 90°$.
- The pressure drop increases with the increase of concentrations of CMC solutions, Re_g, twist element and the decrease of blade length.

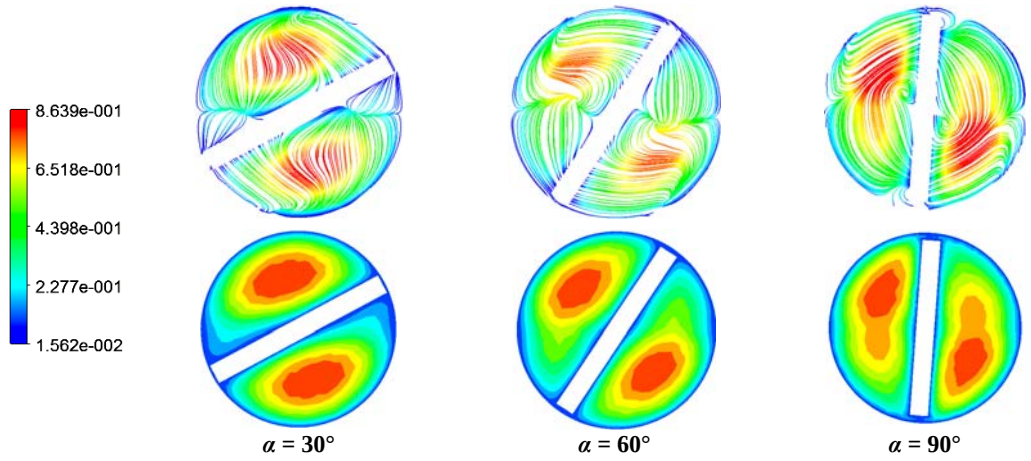

Fig. 17. Streamlines for Re_g = 100, Solution No. 1, l^* = 0.10, X^* = 0.59

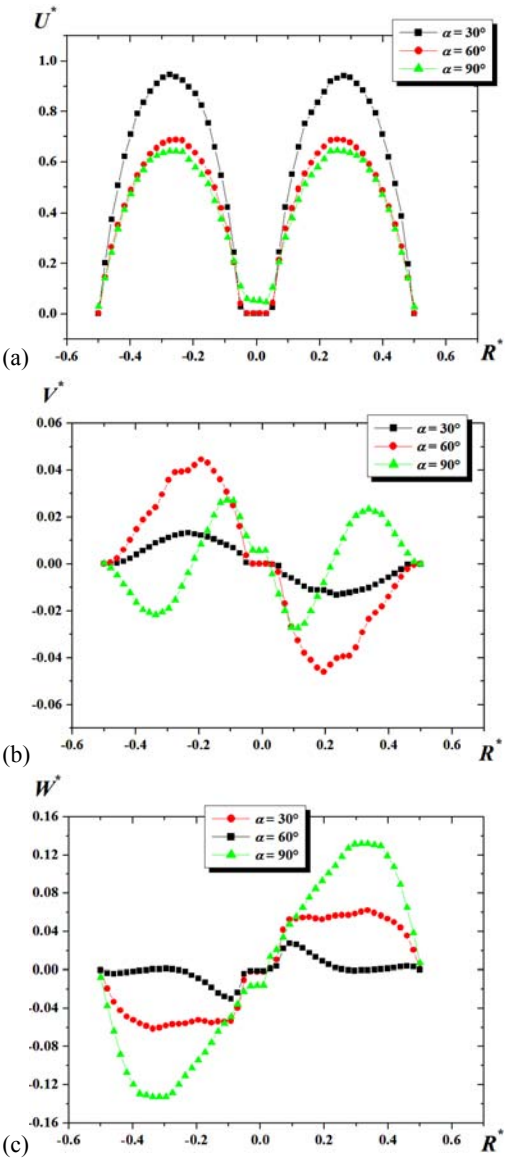

Fig. 18. Velocities vs. mixer radius for Solution No. 1, X^* = 0.50, l^* = 0.10 (a) axial velocity, (b) radial velocity, (c) tangential velocity.

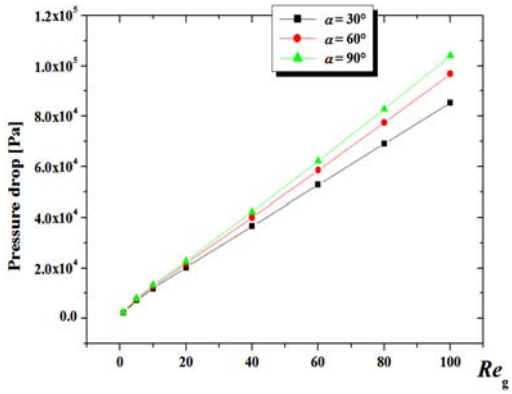

Fig. 19. Pressure drop for different twist angles, Solution No. 1, l^* = 0.10.

REFERENCES

Ameur, H. (2015). Energy efficiency of different impellers in stirred tank reactors. *Energy* 93, 1980-1988.

Ameur, H. (2016a). Effect of some parameters on the performance of anchor impellers for stirring shear-thinning fluids in a cylindrical vessel. *Journal of Hydrodynamics* 28, 669-675.

Ameur, H. (2016b). 3D hydrodynamics involving multiple eccentric impellers in unbaffled cylindrical tank. *Chinese Journal of Chemical Engineering* 24, 572-580.

Barega, E. W., E. Zondervan and A. B. Haan (2013). Influence of physical properties and process conditions on entrainment behavior in a static-mixer settler setup. *Industrial and Engineering Chemistry Research* 52, 2958-2968.

Bi, R., X. Yang, T. Tan and S. Zheng (2013). A method to predict phosgenation reaction performance to produce toluene diisocyanate in jet reactors. *Industrial and Engineering*

Chemistry Research 52, 15353-15358.

Etchells, A. W. and C. F. Meyer (2004). Mixing in pipelines, in: E.L. Paul, V.A. Atiemo-Obeng, S.M. Kresta (Eds.), Handbook of Industrial Mixing, John Wiley & Sons Inc., Hoboken, NJ, 391-475.

Galaktionov, O. S., P. D. Anderson, G. W. M. Peters and H. E. H. Meijer (2003). Mixing and compounding-analysis and optimization of Kenics static mixers. *International Polymer Processing* 18, 138-150.

Ghanem, A., T. Lemenand, D. D. Valle and H. Peerhossaini (2014). Static mixers: Mechanisms, applications, and characterization methods – A review. *Chemical Engineering Research and Design* 92, 205-228.

Gopal, K. I., P. Bhattacharjee and R. Parthasarathy (2015). Effects of shear thinning fluid rheological properties on IMR radius in laminar stirred tanks. *APCChE 2015 Congress incorporating Chemeca 2015, Melbourne, Victoria*, Paper no. 3135026.

Goto, S. and P. D. Gaspillo (1992). The effect of static mixer on mass transfer in draft tube bubble column and in external loop column. *Chemical Engineering Science* 47, 3533-3539.

Grace, C. D. (1971). Static mixing and heat transfer. *Chemical and Process Engineering* 52, 57-59.

Heyouni, A., M. Roustan and Z. Do-Quang (2002). Hydrodynamics and mass transfer in gas–liquid flow through static mixers. *Chemical Engineering Science* 57, 3325-3333.

Hobbs, D. M. and F. J. Muzzio (1997). The Kenics static mixer: a three dimensional chaotic flow. *Chemical Engineering Journal* 67, 153-166.

Hobbs, D. M. and F. J. Muzzio (1998). Effects of injection location flow ratio and geometry on Kenics static mixer performance. *AIChE Journal* 43, 3121-3132.

Hobbs, D. M. and F. J. Muzzio (1998). Optimization of a static mixer using dynamical systems techniques. *Chemical Engineering Science* 53, 3199-3213.

Hobbs, D. M., Swanson, P. D. and F. J. Muzzio (1998). Numerical characterization of low Reynolds number flow in the Kenics static mixer. *Chemical Engineering Science* 53, 1565-1584.

Jin, Y. and Y. Cheng (2011). Chemical engineering in china: past, present and future. *AIChE Journal* 57, 552-560.

Kazemzadeh, A., F. Ein-Mozaffari, A. Lohi and L. Pakzad (2016). Investigation of hydrodynamic performances of coaxial mixers in agitation of yield-pseudoplasitc fluids: Single and double central impellers in combination with the anchor. *Chemical Engineering Journal* 294, 417-430.

Khapre, A. and B. Munshi (2015). Numerical investigation of hydrodynamic behavior of shear thinning fluids in stirred tank. *Journal of the Taiwan Institute of Chemical Engineering* 56, 16-27.

Kroon, M.C. and D. Hartmann (2008). Toward a sustainable chemical industry: cyclic innovation applied to ionic liquid-based technology. *Industrial and Engineering Chemistry Research* 47, 8517-8525.

Kumar, V., V. Shirke and K. D. P. Nigam (2008). Performance of Kenics static mixer over a wide range of Reynolds number. *Chemical Engineering Journal* 139, 284-295.

Li, J. and I. A. Karimi (2011). Scheduling gasoline blending operations from recipe determination to shipping using unit slots. *Industrial and Engineering Chemistry Research* 50, 9156-9174.

Martin, N. and C. Galey (1994). Use of static mixer for oxidation and disinfection by ozone. *Ozone – Science Engineering* 16, 455-473.

Meijer, H. E. H., M. K. Singh and P. D. Anderson (2012). On the performance of static mixers: a quantitative comparison. *Progress in Polymer Science* 37, 1333-1349.

Meng, H., F. Wang and Y. Yu (2014). A numerical study of mixing performance of high-viscosity fluid in novel static mixers with multitwisted leaves. *Industrial and Engineering Chemistry Research* 53, 4084-4095.

Metzner, B. and R. E. Otto (1957). Agitation of non-Newtonian fluids. AIChE Journal 3, 3-11.

Munter, R. (2010). Comparison of mass transfer efficiency and energy consumption in static mixers. *Ozone – Science Engineering* 32, 399-407.

Olmiccia, J., M. Heniche and F. Bertrand (2011). A particulate method for determining residence time in viscous flow processes. *Macromolecular and Material Engineering* 296, 362-372.

Rabha, S., M. Schubert, F. Grugel, M. Banowski and U. Hampel (2015). Visualization and quantitative analysis of dispersive mixing by a helical static mixer in upward co-current gas–liquid flow. *Chemical Engineering Journal* 262, 527-540.

Rafiee, M., M. J. H. Simmons and A. Ingram (2013). Development of positron emission particle tracking for studying laminar mixing in Kenics static mixer. *Chemical Engineering Research and Design* 91, 2106-2113.

Rudman, M., H. M. Blackburn, L. J. W. Grahamand L. Pullum (2004). Turbulent pipe flow of shear-thinning fluids. *Journal of Non-Newtonian Fluid Mechanics* 118, 33-48

Saatdjian, E., A. J. S. Rodrigo and J. P. B. Mota (2012). On chaotic advection in a static mixer.

Chemical Engineering Journal 187, 289-298.

Thakur, R. K., C. Vial, K. D. P. Nigam, E. B. Nauman and G. Djelveh (2003). Static mixers in the process industries – a review. *Chemical Engineering Research and Design* 81, 787-826.

Wilkinson, W. L. and M. J. Cliff (1977). An investigation into the performance of a static in line mixer, in: *Second European Conference on Mixing, BHRA Fluid Engineering, Cambridge* 15–25.

Xu, G., L. Feng, Y. Li and K. Wang (1997). Pressure drop of pseudo-plastic fluids in static mixers. *Chinese Journal of Chemical Engineering* 5, 93-96.

Zhang, L., J. Dong, B. Jiang, Y. Sun, F. Zhang and L. Hao (2015). A study of mixing performance of polyacrylamide solutions in a new-type static mixer combination. *Chemical Engineering and Processing* 88, 19-28.